Estimation of Average Diffuse Aquifer Recharge Using Time Series Modeling of Groundwater Heads

Obergfell, Christophe; Bakker, Mark; Maas, Kees

Important note
To cite this publication, please use the final published version (if applicable).
Please check the document version above.

Estimation of Average Diffuse Aquifer Recharge Using Time Series Modeling of Groundwater Heads

Christophe Obergfell[1] (ID)**, Mark Bakker[1]** (ID)**, and Kees Maas[2]**

[1]Faculty of Civil Engineering and Geosciences, Delft University of Technology, Delft, Netherlands, [2]Maas Geohydrologisch Advies, Middelburg, Netherlands

Abstract A new method is presented to estimate average diffuse aquifer recharge of water table aquifers in temperate climates using time series analysis of water table level fluctuations. An accurate estimate of the recharge caused by rainfall requires an accurate estimate of the influence of evaporation. In temperate climates, evaporation imprints a seasonal component in the water table fluctuations. As such, recharge is estimated from time series models fitted to observed heads under the additional constraint that the seasonal harmonic of the observed head is reproduced as the sum of the transformed seasonal harmonics present in precipitation, evaporation, and pumping. An explicit equation is presented, in terms of the model parameters, for the damping and phase shift of the response to the seasonal harmonic of the stresses. Taking into account the seasonal harmonic of the observed heads results in more reliable recharge estimates compared to standard time series analysis. The method is limited to systems that are sufficiently linear and that remain unaltered over the analysis period. Head fluctuations and stresses should contain a seasonal harmonic that can be estimated with accurately. Runoff must be negligible or quantifiable. The method is applied to measured heads obtained from piezometers situated on and around the ice-pushed sand ridge of Salland in the Netherlands and compares well with recharge estimates based on the saturated zone chloride mass balance.

1. Introduction

Natural groundwater recharge, the replenishment of aquifers from precipitation, is one of the major subjects of investigation in hydrology but still remains a difficult component to estimate in the water balance of an area (e.g., Bakker et al., 2013; Healy, 2012). A large number of techniques exist to try to quantify groundwater recharge for various time and space scales (Healy & Cook, 2002); each technique requires different input data, from simple head measurements to detailed hydrochemistry. Scanlon et al. (2002) review the various techniques and propose an iterative approach to recharge estimation, refining the estimates as additional data are gathered. A wide variety of approaches is recommended in order to increase the confidence in recharge estimates. The topic of this paper is to add a new approach to estimate average diffuse aquifer recharge over large time periods (years to tens of years). It is based on time series analysis of measured head variations combined with measured stresses on the aquifer, including rainfall, reference evaporation, and pumping.

One approach to estimate recharge from measured head variations and rainfall is the water table fluctuation method. In its original form, it is applicable to short-term water level rises that occur in response to individual storm events (Healy, 2012; Healy & Cook, 2002; Meinzer, 1923), neglecting the slow but continuous water table recession that may take place in response to previous recharge events. Recent developments aimed at applying the water-table fluctuation method over longer time periods, while systematically taking into account the effect of aquifer drainage and cumulating the effect of successive rain events. This can be achieved using the master recession curve method (Heppner & Nimmo, 2005; Nimmo et al., 2015), either by quantifying the drainage intensity (Crosbie et al., 2005), or by using an analytical groundwater model (Cuthbert, 2010). In all these methods, identification of the drainage parameters and the specific yield remain a challenge.

In groundwater hydrology, time series analysis has been used primarily to model and predict groundwater heads. Different methods are employed: transfer function noise models of the Box and Jenkin's type (e.g., Baggelaar, 1988; Gehrels et al., 1994; van Geer & Zuur, 1997), models based on the convolution of response functions (e.g., Manzione et al., 2012; Peterson & Western, 2014; von Asmuth et al., 2002), or physically

based models (e.g., Berendrecht et al., 2006). A common issue in many of these methods is the correlation between model parameters that determine the influence of evaporation and pumping (e.g., Shapoori et al., 2015). Equally good fits of the observed heads can be obtained when, for example, the effects of groundwater pumping are compensated by the effects of evaporation, or vice versa (Shapoori et al., 2015). This problem of equifinality is undesirable, especially when the model parameters are intended to be used to quantify physical quantities like groundwater recharge (e.g., Beven, 1993).

The objective of this paper is to estimate time-averaged groundwater recharge using time series analysis of groundwater heads. A reliable estimate of the recharge requires an accurate identification of the influence of evaporation on groundwater head fluctuations. In temperate climates, evaporation, more than any other stress, dictates the seasonal behavior of the water table fluctuation. It stands to reason that if two parameter sets of a time series model give a similar fit, the evaporation is better estimated by the parameter set that matches the seasonal behavior better. The seasonal behavior of the water table can be characterized by the sinusoidal component with a period of 1 year, referred to here as the seasonal harmonic. The approach presented in this paper uses the seasonal harmonic as an additional signature that is implemented in the form of a model optimization constraint. The inclusion of multiple signatures of the hydrological response when calibrating a model is also applied in other parts of hydrology (e.g., Euser et al., 2013; Hrachowitz et al., 2014; Koutsoyiannis, 2010).

This paper is organized as follows. First, time series analysis by the method of predefined response functions is reviewed briefly. Second, equations are derived for the seasonal harmonic response caused by rainfall, evaporation, and pumping; these equations are used as a constraint when estimating the time series model parameters. Third, a case study is presented to demonstrate the efficacy of the presented approach. In the discussion, recharge estimates obtained with the proposed approach are compared to results from standard time series analysis where the seasonal harmonic is not used as a constraint, recharge estimates for time periods with different mean heads are compared, and the possible effects of the uncertainty in the seasonal harmonic are discussed. Finally, the estimated long-term recharge is compared with an estimate obtained from the saturated zone chloride mass balance method.

2. Methods

2.1. Time Series Analysis With Predefined Response Functions

The method of time series analysis with predefined response functions is described in several papers (e.g., Obergfell et al., 2016; Peterson & Western, 2014; von Asmuth et al., 2002). It is briefly reviewed here. The head fluctuations $\varphi(t)$ due to stress time series $q(t)$ at a point in space is obtained by convolution of $q(t)$ with the corresponding impulse response function $\theta(t)$:

$$\varphi(t) = \int_0^t q(\tau)\theta(t-\tau)d\tau \tag{1}$$

where t is time. In this paper, $\varphi(t)$ is used for the head fluctuation caused by one specific stress, while $h(t)$ is used for the head fluctuation caused by the superposition of all stresses. The dependence of the response function on spatial coordinates is omitted in this notation. $\theta(t)$ has the shape of the response of the groundwater head to an instantaneous stress event of unit strength (for example, an instantaneous shower of unit height). The dimension of $\theta(t-\tau)$ is determined by the dimension of the stress so that the product $q(\tau)\theta(t-\tau)$ has the dimension length, like heads.

Stress time series are commonly piecewise continuous (daily rainfall, for example), while response functions are continuous, so that relation (1) needs to be modified as follows. The unit step response function $s(t)$ is obtained from the impulse response function $\theta(t)$ as

$$s(t) = \int_0^t \theta(t-\tau)d\tau \tag{2}$$

The step response function has the dimension of length per dimension of stress. From the step response function, the block response function is derived as

$$\psi(t, \Delta t) = s(t) - s(t - \Delta t) \tag{3}$$

and represents the response to a unit stress distributed uniformly from $t = 0$ to $t = \Delta t$. Time is discretized in stress periods, where Δt_i is the length of stress period i. Stress q_i is approximated as uniform over stress period i from $t = t_i - \Delta t_i$ to $t = t_i$. The head at time t_i is obtained by summing the effects at time t_j of all past stress periods

$$\varphi(t_j) = \sum_{i=1}^{j} q_i \psi(t_j - t_{i-1}, \Delta t_i) \tag{4}$$

where

$$t_j = \sum_{i=1}^{j} \Delta t_i \tag{5}$$

This is a discrete form of convolution. Alternatively, the series $\varphi(t_i)$ can be seen as a weighted moving average of the series q, ψ being the weighting function. The modeled heads $h(t)$ are obtained by adding the contributions of all stresses $\varphi_i(t)$ plus a reference level

$$h(t) = \sum_i \varphi_i(t) + d \tag{6}$$

where d is called the drainage base here.

The observed heads $h_o(t)$ are equal to the modeled heads plus a residual $r(t)$:

$$h_o(t) = \sum_i \varphi_i(t) + d + r(t) \tag{7}$$

Autocorrelation in the residuals is removed by modeling them with an exponential decay process (von Asmuth & Bierkens, 2005). The residual at time t_i is related to the residual at time t_{i-1} as

$$r(t_i) = r(t_{i-1}) \exp(-\alpha(t_i - t_{i-1})) + n(t_i) \tag{8}$$

where α is the residual decay factor and $n(t_i)$ represents approximate white noise.

Three types of stresses are considered here to simulate head fluctuations: precipitation, evaporation, and pumping. The impulse response function considered for these stresses is a scaled gamma distribution:

$$\theta(t) = M \frac{a^n t^{n-1}}{\Gamma(n)} e^{-at} \tag{9}$$

where M is a scaling factor, a and n define the shape of the function, and $\Gamma(n)$ is the gamma function of n. This response function is commonly applied for precipitation and evaporation (e.g., von Asmuth et al., 2012). It is also appropriate to simulate the slow response to pumping in a phreatic aquifer when piezometers are not in the direct vicinity of the pumping wells. The corresponding step response function(t) is a scaled incomplete gamma function of the form:

$$s(t) = \frac{M}{\Gamma(n)} \int_0^t a^n \tau^{n-1} e^{-a\tau} d\tau = M\Gamma(n, at) \tag{10}$$

where $\Gamma(n, at)$ is the lower incomplete gamma function of n and at (e.g., Abramowitz & Stegun, 1964). The parameters M, a, and n are referred to here as the first, second, and third parameters of the incomplete gamma function.

The observed heads and stresses are written with respect to their means, so that (7) becomes

$$h_o(t) - \overline{h}_o = \sum_i (\varphi_i(t) - \overline{\varphi}_i) + d - \overline{h}_o + \sum_i \overline{\varphi}_i + r(t) \tag{11}$$

The drainage base is set equal to the mean observed head $\overline{h}_o$ minus the sum of the mean contributions of the stresses (similar to von Asmuth et al., 2002)

$$d = \overline{h}_o - \sum_i \overline{\varphi}_i \tag{12}$$

so that

$$h_o(t) - \overline{h}_o = \sum_i (\varphi_i(t) - \overline{\varphi}_i) + r(t) \tag{13}$$

The mean response $\overline{\varphi}_i$ to stress i is computed, using (9) as the response function, as

$$\overline{\varphi}_i = \overline{q}_i \int_0^{\infty} \theta_i(t-\tau)d\tau = \overline{q}_i M_i \tag{14}$$

The scaling parameter M_i corresponds to the final response of the groundwater head when stress i is applied continuously with unit intensity.

2.2. Estimation of the Mean Recharge

In this study, the responses to precipitation and to reference evaporation are assumed to have the same shape, sharing the same parameters a and n defined in (9), and differ only by their final response magnitudes M_p and M_e, respectively. The ratio of the magnitudes is called f

$$f = \frac{M_e}{M_p} \tag{15}$$

further referred to as the evaporation factor.

In the absence of runoff, R represents the diffuse, time-averaged groundwater recharge, approximated as precipitation minus all forms of evaporation, which is the sum of interception, transpiration, and soil evaporation, expressed by the relation:

$$R = P - fE \tag{16}$$

where P and E are measured precipitation and measured reference evaporation $[LT^{-1}]$, respectively. Possible seasonal dependence of the evaporation factor is not taken into account. The passage through the unsaturated zone is taken into account by the response to recharge, which mimics a dispersion process (Besbes & de Marsily, 1984; Gehrels et al., 1994).

2.3. Seasonal Harmonic

Accurate identification of the influence of evaporation on head fluctuations is a crucial requirement for a reliable estimation of the recharge. In the proposed method, this is achieved by taking the best estimate of the seasonal harmonic of the observed heads into account as an additional signature. The seasonal behavior is represented by the seasonal harmonic component $y(t)$ defined as

$$y = A\sin(\omega(t-T)) \tag{17}$$

where A is the amplitude, T is the phase shift (in days), and ω is $2\pi/365.25(day^{-1})$. Since ω is already known, the parameters A and T of a measured time series can be determined with a least squares procedure. A discrete Fourier transformation of the signals using, for example, a fast Fourier transform scheme is an equivalent alternative if all time series are available at equidistant points in time.

Convolution of the seasonal harmonic of a stress time series with amplitude A_s and phase shift T_s with an impulse response function $\theta(t)$ results in a seasonal harmonic with a transformed amplitude $\widetilde{A}_s$ and a phase shift $\widetilde{T}_s$, as demonstrated in Appendix A:

$$\widetilde{y}(t) = \int_0^{\infty} A_s \sin(\omega(t-\tau-T_s))\theta(\tau)d\tau = \widetilde{A}_s \sin\left(\omega\left(t-\widetilde{T}_s\right)\right) \tag{18}$$

When the scaled gamma function (9) is used for the impulse response function $\theta(t)$, the amplitude ratio $\widetilde{A}_s/A_s$ and phase shift Δt_s are (Appendix A)

$$\frac{\widetilde{A}_s}{A_s} = \frac{M_s}{\left(1 + \frac{\omega}{a_s}^2\right)^{\frac{n_s}{2}}} \tag{19}$$

$$\Delta t_s = \widetilde{T}_s - T_s = \frac{n_s}{\omega} \arctan \frac{\omega}{a_s} \tag{20}$$

Addition of the seasonal harmonics of the responses to precipitation (amplitude $\widetilde{A}_p$ and phase shift) and evaporation (amplitude $\widetilde{A}_e$ and phase shift) results in a new seasonal harmonic given by

$$\widetilde{A}_p \sin\left(\omega\left(t - \widetilde{T}_p\right)\right) + \widetilde{A}_e \sin\left(\omega\left(t - \widetilde{T}_e\right)\right) = \widetilde{A}_2 \sin\left(\omega\left(t - \widetilde{T}_2\right)\right) \tag{21}$$

where amplitude $\widetilde{A}_2$ and phase shift $\widetilde{T}_2$ are given by

$$\widetilde{A}_2 = \sqrt{\widetilde{A}_p^2 + \widetilde{A}_e^2 + 2\widetilde{A}_p\widetilde{A}_e \cos(\omega(T_e - T_p))} \tag{22}$$

$$\widetilde{T}_2 = \frac{1}{\omega} \arctan\left(\frac{\widetilde{A}_e \sin(\omega(T_e - T_p))}{\widetilde{A}_p + \widetilde{A}_e \cos(\omega(T_e - T_p))}\right) + \widetilde{T}_p \tag{23}$$

where Δt_p is the time delay between the seasonal harmonic of the measured time series of precipitation and the seasonal harmonic of the response to precipitation, calculated by relation (20). In the derivation of (22) and (23) it is used that $\widetilde{T}_e - \widetilde{T}_p = T_e - T_p$, which holds because $\Delta t_e = \Delta t_p$ and the response of precipitation and evaporation have the same parameters a and n (see equation (20)).

Addition of the seasonal harmonics of the combined response to precipitation and evaporation (amplitude $\widetilde{A}_2$ and phase shift) to the seasonal harmonic of the response to pumping (amplitude $\widetilde{A}_w$ and phase shift $\widetilde{T}_w$) results in a new seasonal harmonic with amplitude $\widetilde{A}_3$ and phase shift $\widetilde{T}_3$ given by

$$\widetilde{A}_3 = \sqrt{\widetilde{A}_2^2 + \widetilde{A}_w^2 + 2\widetilde{A}_w\widetilde{A}_2 \cos\left(\omega\left(\widetilde{T}_w - \widetilde{T}_2\right)\right)} \tag{24}$$

$$\widetilde{T}_3 = \frac{1}{\omega} \arctan\left(\frac{\widetilde{A}_w \sin\left(\omega\left(\widetilde{T}_w - \widetilde{T}_2\right)\right)}{\widetilde{A}_w + \widetilde{A}_2 \cos\left(\omega\left(\widetilde{T}_w - \widetilde{T}_2\right)\right)}\right) + \widetilde{T}_2 \tag{25}$$

where Δt_w is the time delay between the seasonal harmonic of the measured pumping time series and the seasonal harmonic of the response to pumping.

The amplitude A_h and phase shift T_h of the seasonal harmonic of the measured heads is set equal to the sum of the seasonal harmonics of the responses of all stresses in the time series model. When precipitation and evaporation are the only stresses, this gives the constraint

$$\begin{cases} A_h = \widetilde{A}_2 \\ T_h = \widetilde{T}_2 \end{cases} \tag{26}$$

When pumping is also included, this gives the constraint

$$\begin{cases} A_h = \widetilde{A}_3 \\ T_h = \widetilde{T}_3 \end{cases} \tag{27}$$

2.4. Parameter Estimation

The time series model is fitted to the available observed heads as given in (13), under the constraints (26) or (27). Parameter optimization is performed by minimizing the objective function $S(\mathbf{p})$ defined as half of the sum of the squared noise terms n_i defined in (8):

$$S(\mathbf{p}) = \frac{1}{2} \sum_{i=1}^{N_o} n_i^2 \tag{28}$$

where N_o is the number of observations, $\mathbf{p}$ is the vector of N_p model parameters, corresponding to the parameters of the scaled incomplete gamma function of each response function as defined in (10) plus the noise decay parameter as defined in (8). The search for the minimum of the objective function is performed using a modified Gauss-Newton algorithm (e.g., Hill, 1998) starting from initial values selected by applying a preliminary Latin Hypercube sampling of the parameters space (Iman et al., 1981). Note that starting the optimization from different initial parameter values does not affect the estimation outcome, suggesting the identification of a global optimum.

The constraints (26) or (27) constitute a system of nonlinear equations solved at each iteration of the optimization process for parameters n_p and f applying the modified Powell method, implemented in the MINPACK routines package (Moré et al., 1980), and called from the open-source Python package Scipy (Jones et al., 2001). The constraints imposed on the model parameters limit the search for the optimal parameters to a subregion that is unlikely to contain the optimum of the unconstrained models, but it corresponds to parameters sets that lead to models that are physically more realistic.

The covariance matrix $\mathbf{C}$ of the logarithm of the optimized parameters is approximated as (e.g., Yuen, 2010):

$$\mathbf{C} = \sigma^2 \mathbf{H}^{-1} \tag{29}$$

where $\mathbf{H}$ is the Hessian of the objective function and σ^2 is the variance of the noise. The Hessian is approximated as $\mathbf{H} \simeq \mathbf{J}^T\mathbf{J}$, where $\mathbf{J}$ is the Jacobian matrix. Confidence intervals of optimized parameters are estimated assuming a Normal distribution around the optimum, scaled by the variance of the parameter as given by the covariance matrix. For an optimal value $\ln(p_i)$ of log-transformed parameter p_i, the lower and upper limits of the 95% confidence interval are

$$\ln(p_i) \pm 1.96 \sigma_{\ln(pi)} \tag{30}$$

The confidence intervals of the back-transformed parameters are obtained by taking the exponential of the lower and upper bounds of the log-transformed parameters. The confidence interval of the estimated recharge is computed using Monte Carlo simulations of parameters M_p and a_p based on the covariance matrix of the optimized time series models. For each realization, parameters n_p and f are obtained by the constraints described in section 2.3, using the approach described above. Recharge is inferred from parameter f by applying relation (16). The confidence intervals are therefore consistent with constraints (26) and (27).

3. Site Description

3.1. Hydrogeology

The proposed method is applied to a field site in the ice-pushed ridge of Salland, in the Dutch province of Overijssel, in the vicinity of a drinking water supply well field (Figure 1).

Ice-pushed ridges, also referred to as push moraines, build up at the margin of glaciers. The ice-pushed ridge of Salland was formed during the second to last ice age called the Saalian ice age, from about 200,000 to 130,000 years ago. This period corresponds to the southernmost advance of the ice sheet in Northern Europe during the Pleistocene time. The highest elevation point of the ridge is about 60 m above NAP (the datum used in the Netherlands).

Ice-pushed ridges consist of thrust sheets, the strikes of which generally dip 30-40° toward a glacial basin. In the Netherlands, the thrust sheets consist mainly of sandy formations with possible intercalations of less permeable formations. This internal structure can result in an anisotropic permeability field, which is difficult to simulate in a groundwater model due to its heterogeneous character. In Salland, the strike direction is north-south with thrusts dipping to the west.

Both sides of the sand ridge are drained areas corresponding to former water-logged bogs. These zones have been drained in the Middle Ages and are now flat meadows drained by a network of small canals and ditches

Figure 1. Field site location.

(Figure 2). The vegetation on the ridge consists of heather, grassland, deciduous trees, and rather sparse coniferous woods.

3.2. Data

Measurements at five piezometers are analyzed. The location of the piezometers is shown in Figure 2. Their characteristics are listed in Table 1. Heads were recorded twice a month. In the second half of the 1990s, the head fluctuation regime changes as a result of massive dredging works in the main river draining the aquifer investigated. Time series analysis is therefore performed up to that moment, over the period 1982–1995, which is a period for which measurements are available for all piezometers except piezometer 2 for which data were only available after 1984.

Daily precipitation and reference evaporation are obtained from the Royal Netherlands Meteorological Institute. The reference evaporation is Makkink reference evaporation, defined as the evaporation of well-watered short grass on a regional scale (De Bruin, 1987). Precipitation was measured at the meteorological station of Hellendoorn (Figure 2). Daily reference evaporation, which varies much less in space than precipitation, was measured at the meteorological station of de Bilt, about 85 km to the south-west of the field site. A drinking water production well field is in operation on the ridge of Salland since 1954, with pumping records available from 1974 onward. The average groundwater extraction is 5.10^6 m^3/year. The location of the well field is shown in Figure 2.

The stress time series and the corresponding seasonal harmonics are plotted in Figure 3, together with the hydrographs of piezometers 1 and 3. As the parameters of the response to separate wells could not be identified, the combined discharge of all wells was added in one stress time series, which is a common approximation. The combined pumping time series shows a significant trend, but no significant difference was found between the seasonal harmonics of the pumping time series estimated before and after detrending so detrending was omitted here. Piezometer 1 is a relatively shallow well with a faster reaction to recharge, while piezometer 3 is a deeper well with a slower reaction to recharge.
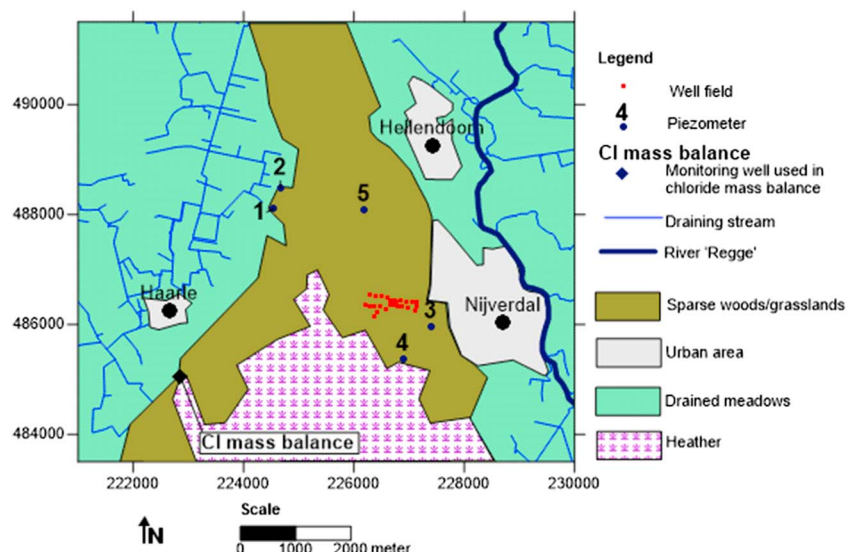

Figure 2. Field site.

Table 1
Piezometers Analyzed to Estimate Groundwater Recharge

Piezometer number	Piezometer id	X coordinate (m)	Y coordinate (m)	Screen level (m NAP)	Surface elevation (m NAP)	Median observed heads (m NAP)	Distance to middle of well field (m)
1	28AP0093	224,550	488,100	2.10	11.60	9.24	2,750
2	28AL0019	224,668	488,474	8.07	10.32	9.15	2,900
3	28CP0197	227,398	485,958	4.70	15.26	8.52	825
4	28CP0204	226,894	485,364	2.83	21.26	9.59	1,025
5	28AP0134	226,181	488,081	−2.50	22.40	8.46	1,800

4. Results

4.1. Model Parameters and Recharge

The proposed time series modeling approach is applied to the five piezometers given in Table 2. For each piezometer, the nine model parameters are fitted, of which two parameters are obtained from the constraint
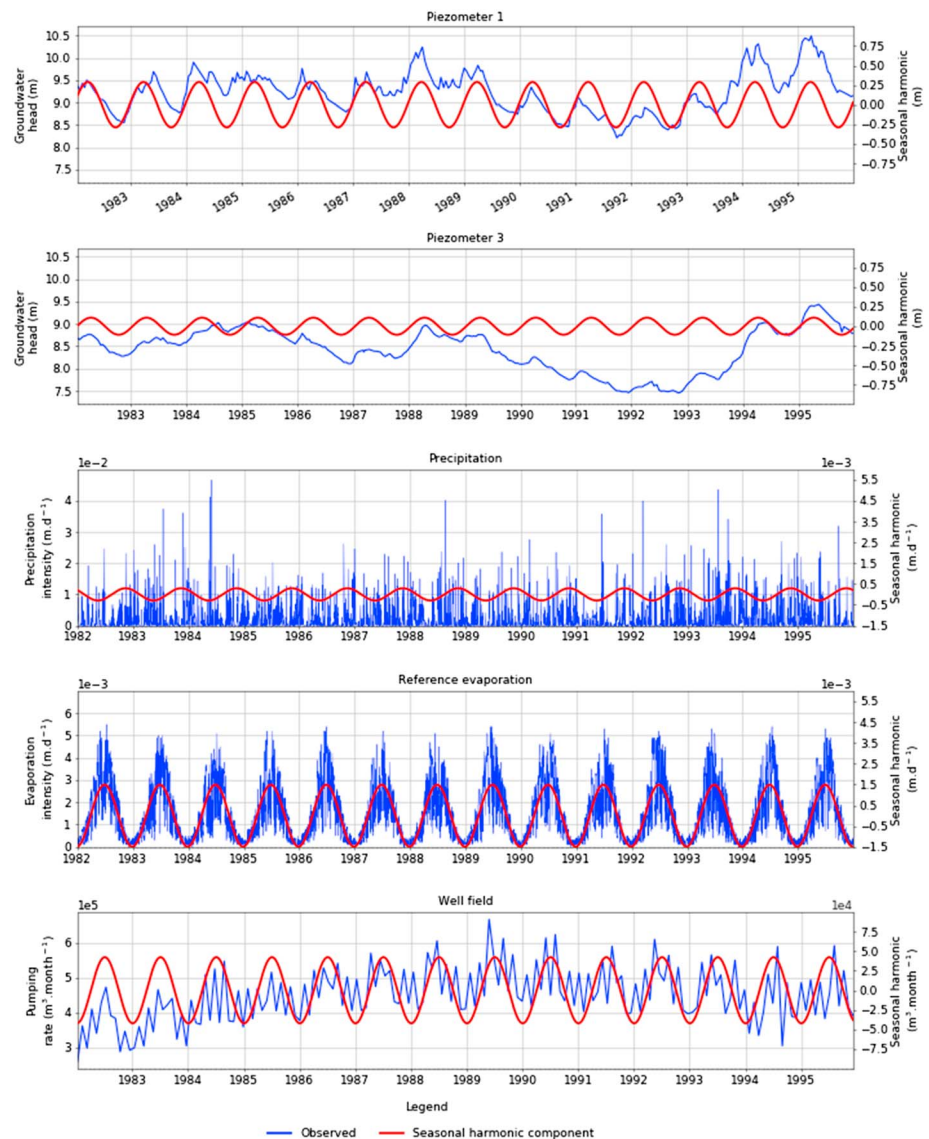
Figure 3. Observed heads in piezometers 1 and 3 and stresses (blue) with their seasonal harmonic component (red lines and right axis).

Table 2
Estimated Parameters With 95% Confidence Intervals for Models Optimized Under Constraints (26) or (27)

Symbol	Unit	Estimated parameters values per piezometer				
		1	2	3	4	5
$M_p \times 10e^3$	m	1.56 [1.51,1.60]	1.53 [1.48,1.59]	2.09 [2.05,2.12]	2.17 [2.12,2.22]	1.80 [1.75,1.82]
$a_p \times 10e^{-3}$	day^{-1}	2.37 [2.30,2.44]	1.93 [1.84,2.02]	2.43 [2.40,2.47]	3.29 [3.24,3.35]	4.42 [4.34,4.50]
n_p[a]	-	1.11 [1.11,1.12]	0.97 [0.96,0.98]	1.55 [1.54,1.56]	2.02 [2.01,2.03]	2.41 [2.40.2.42]
f[a]	-	1.03 [1.01,1.05]	0.97 [0.95,0.99]	0.67 [0.65,0.68]	0.73 [0.71,0.74]	0.88 [0.87,0.88]
$M_w \times 10e^{-4}$	m	-	-	1.34 [1.30,1.38]	1.12 [0.90,1.14]	-
$a_w \times 10e^{-4}$	day^{-1}	-	-	1.37 [1.21,1.56]	0.96 [0.64,1.42]	-
n_w	-	-	-	1.06 [0.97,1.16]	1.13 [1.11, 1.58]	-
$\alpha \times 10e^{-2}$	day^{-1}	4.31 [3.65,5.14]	5.78 [4.65,7.21]	0.73 [0.54,0.98]	0.26 [0.22,0.95]	1.80 [1.59,2.03]
d[b]	m above datum	8.05	7.87	7.62	8.47	6.57[c]

Note. M_p, a_p, and n_p are the first, second, and third parameters of the response function to precipitation; M_w, a_w, and n_w are the first, second, and third parameter, of the response function to pumping; f is the evaporation factor; α is the exponential decay factor of the noise model; and d is the drainage base.
[a]Inferred from constraints (19) and (20). [b]Relation (12). [c]Sum of pumping effects and drainage base.

on the seasonal harmonic and the drainage base d is computed with (12). The effect of pumping was negligible for piezometers 1 and 2, so that only six parameters were fitted. The observed and modeled head fluctuations are shown in Figure 4. The optimal parameters, together with their 95% confidence intervals, are presented in Table 2. The corresponding recharge estimates are given in Table 3.

The goodness of fit of the time series models is expressed as the Nash-Sutcliffe coefficient (Nash & Sutcliffe, 1970) defined as

$$\mathrm{NS} = 1 - \frac{\sum_{i=1}^{N_o} \left(h_{m,i} - h_{o,i}\right)^2}{\sum_{i=1}^{N_o} \left(h_{o,i} - \overline{h}_o\right)^2} \tag{31}$$

where N_o is the number of observed heads, $h_{m,\,i}$ is the modeled head at time i, $h_{o,\,i}$ is the observed head at time i, and $\overline{h}_o$ is the mean observed head. The Nash-Sutcliffe coefficient exceeds 90% for all piezometers, which indicates good fits of the observed heads. Besides the Nash-Sutcliffe coefficient, the standard diagnostic checks on model errors were applied. The resulting noise $n(t)$, defined in (8), is uncorrelated with a distribution close to normal.

5. Discussion

5.1. Estimated Groundwater Recharge

The estimated recharge values for piezometers 1 and 2 represent shallow water table conditions (resp. 0.250 and 0.296 m/year) and are lower than the recharge estimated for piezometers 3 and 4 (resp. 0.447 and 0.416 m/year), representing deep water table conditions. Shallow water tables are favorable for evaporation and transpiration (Doble & Crosbie, 2017), which can explain this difference. Different vegetation covers constitute a second explanation. In particular, the extended heather field near piezometers 3 and 4 favor water table replenishment.

Piezometer 5 lies on the sand ridge and characterizes deep water table conditions, like piezometers 3 and 4. Identification of the pumping influence is difficult in this piezometer due to the relatively large distance (1,800 m) from the center of the well field. The heads measured in this piezometer have consequently been simulated without pumping influence. The effect of pumping at this piezometer is relatively constant and included in the drainage base.

5.2. Comparison With Standard Time Series Analysis

In this paper, groundwater recharge is estimated with time series models where parameters are fitted with the constraint that the observed seasonal harmonic matches the sum of the seasonal harmonics of the
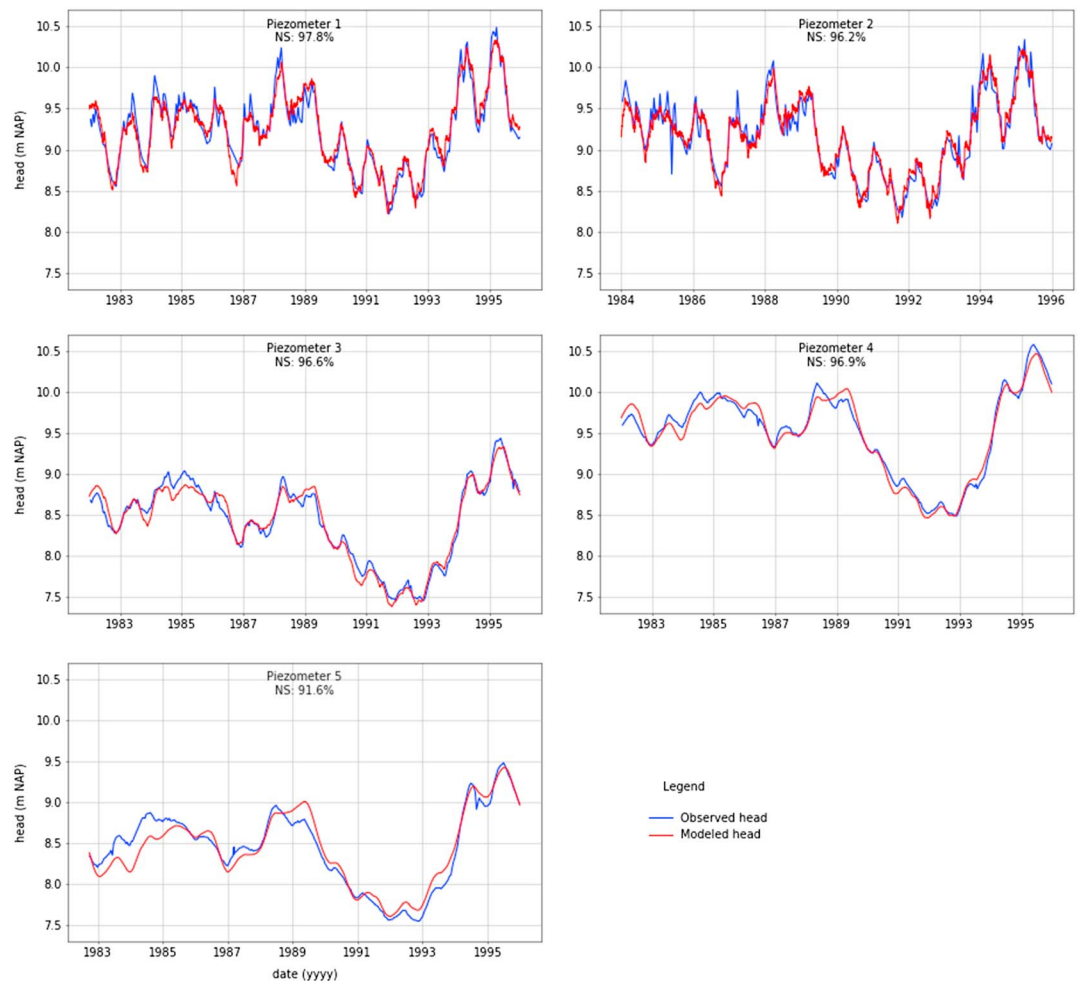
Figure 4. Observed heads (blue) and modeled heads (red) of the five piezometers, with corresponding Nash-Sutcliffe coefficients.

stresses after transformation by the convolution relations of the time series model. This constraint distinguishes the proposed approach from standard time series. The model parameters obtained by the proposed method are expected to provide more reliable estimates of the mean groundwater recharge. The proposed approach is compared to the standard approach for piezometers 1 and 3. The results are given in Table 4.

In both cases, the fits in terms of Nash-Sutcliffe coefficients are similar. In contrast, the model parameters estimated with the proposed method lead to lower recharge estimates for piezometer 1 and 3. The difference between both approaches regarding the modeling of the seasonal harmonic is illustrated in Figure 5 for piezometers 1 and 3. The two graphs at the top show the seasonal harmonic of the observed heads and the seasonal harmonic calculated with the proposed method and the standard method. The seasonal harmonic modeled with the proposed method matches the seasonal harmonic of the observed heads exactly, while the seasonal harmonic modeled with the standard method shows a clear discrepancy. The other graphs in Figure 5 show the stress-specific seasonal harmonics calculated with the proposed and standard methods.

Table 3
Estimated Mean Yearly Recharge for Period 1982–1995 Based on the Optimized Seasonal Harmonic Under Constraints ((26)) or ((27))

Piezometer	1	2	3	4	5
R (m/year)	0.250 [0.243,0.256]	0.296[a] [0.286,0.306]	0.447 [0.440,0.454]	0.416 [0.406,0.421]	0.333 [0.329,0.337]

[a]For period 1984 to 1995.

Table 4
Comparison of Proposed Approach With Standard Time Series Analysis

	Piezometer 1 Standard method	Piezometer 1 Proposed method	Piezometer 3 Standard method	Piezometer 3 Proposed method
Nash-Sutcliffe %	94.7	97.8	96.9	96.5
$M_p \times 10e^3$	1.62 [1.56,1.68]	1.56 [1.51,1.60]	2.19 [2.08,2.31]	2.09 [2.05,2.12]
$a_p \times 10e^{-3}$	2.18 [2.05,2.32]	2.37 [2.30,2.44]	2.26 [2.13,2.41]	2.43 [2.40,2.47]
n_p	1.07 [1.05,1.09]	1.11 [1.11,1.12]	1.51 [1.49,1.54]	1.55 [1.54,1.56]
f	0.92 [0.88,0.97]	1.03 [1.01,1.05]	0.54 [0.65,0.68]	0.67 [0.65,0.68]
$M_w \times 10e^{-4}$	-	-	1.39 [1.34,1.44]	1.34 [1.30,1.38]
$a_w \times 10e^{-4}$	-	-	1.17 [0.98,1.44]	1.37 [1.21,1.56]
n_w	-	-	1.17 [0.98,1.44]	1.06 [0.97,1.16]
α (day^{-1}) $\times 10e^{-2}$	7.06 [5.94,8.52]	4.31 [3.65,5.14]	2.71 [2.34,3.17]	0.73 [0.54,0.98]
d (m NAP)	7.76	8.05	7.14	7.62
R (m/year)	0.306 [0.282,0.332]	0.250 [0.243,0.256]	0.515 [0.501,0.531]	0.447 [0.440,0.454]

The largest difference is caused by the amplitude of the seasonal harmonic of the response to evaporation, as expected.

5.3. Mean Recharge for Different Time Periods

The mean recharge for a period of multiple years depends on the specific time period unless the period is very long. It is expected that the estimated recharge is lower for a multiyear period with a relatively low mean head, while the estimated recharge is expected to be higher for a multiyear period with a relatively high mean head. In fact, if the draining resistance of the aquifer remains constant, a linear relation is expected between the estimated mean recharge for a period and the mean groundwater head for that same period. To test this hypothesis, the mean recharge is estimated for several multiyear periods. Each investigated period is a multiple of whole years in order to equally represent all seasons. Furthermore, the heads at the beginning and end of the period do not deviate more than 0.2 m so that the mean head is a reasonable representation of the head in the period, and the period contains a balanced number of head rises and head declines. Each selected time period is at least 3 years long for the fast head fluctuations (piezometers 1 and 2) and 5 years for the slow head fluctuations (piezometers 3–5).

Time periods conforming to the above stated conditions were generated with a computer script. When two intervals share the same mean head ($\pm$0.05 m), the longest interval is used.

In this fashion, eight time periods were identified for piezometer 1 and seven time periods for piezometer 3. The mean recharge is estimated for each period with the proposed method and is plotted versus the mean head in the corresponding period in Figure 6. Linear regression lines can be fitted through the estimates obtained with the proposed method with an r^2 of 0.94 for piezometer 1 and 0.96 for piezometer 3. Note that for piezometer 5, no significant regression line could be found (not shown).

5.4. Uncertainty of Constraints

The main idea of the proposed method is that a better estimate of the recharge is obtained with time series analysis when the best estimate of the seasonal component of the measured heads is equal to the sum of the responses of the best estimates of the seasonal components of the stresses. It is shown, for the case study, that the proposed approach leads to more reasonable estimates of the recharge with narrower confidence intervals than the standard approach without the constraint.

The question arises whether the proposed method can be further improved. In the proposed method, the best estimates of the seasonal harmonics of the measured heads and measured stresses are used. The uncertainty of these estimates is presented in Table 5. The relative uncertainty of the seasonal harmonics of the heads is smaller for piezometers 1 and 2 than for the other piezometers. For the stresses, the relative uncertainty of the seasonal harmonic of the evaporation is the smallest, while it is the largest for the precipitation. This is encouraging, as the evaporation has the largest influence on the seasonal variation of the head.

A better estimate of the recharge may be obtained when the uncertainty in the seasonal harmonics is taken into account during the parameter estimation process. One way to do this is to perform parameter estimation with a multiobjective function where both the objective function (28) and the constraint (26) or (27) are minimized simultaneously (e.g., Efstratiadis & Koutsoyiannis, 2010). Another approach is to estimate
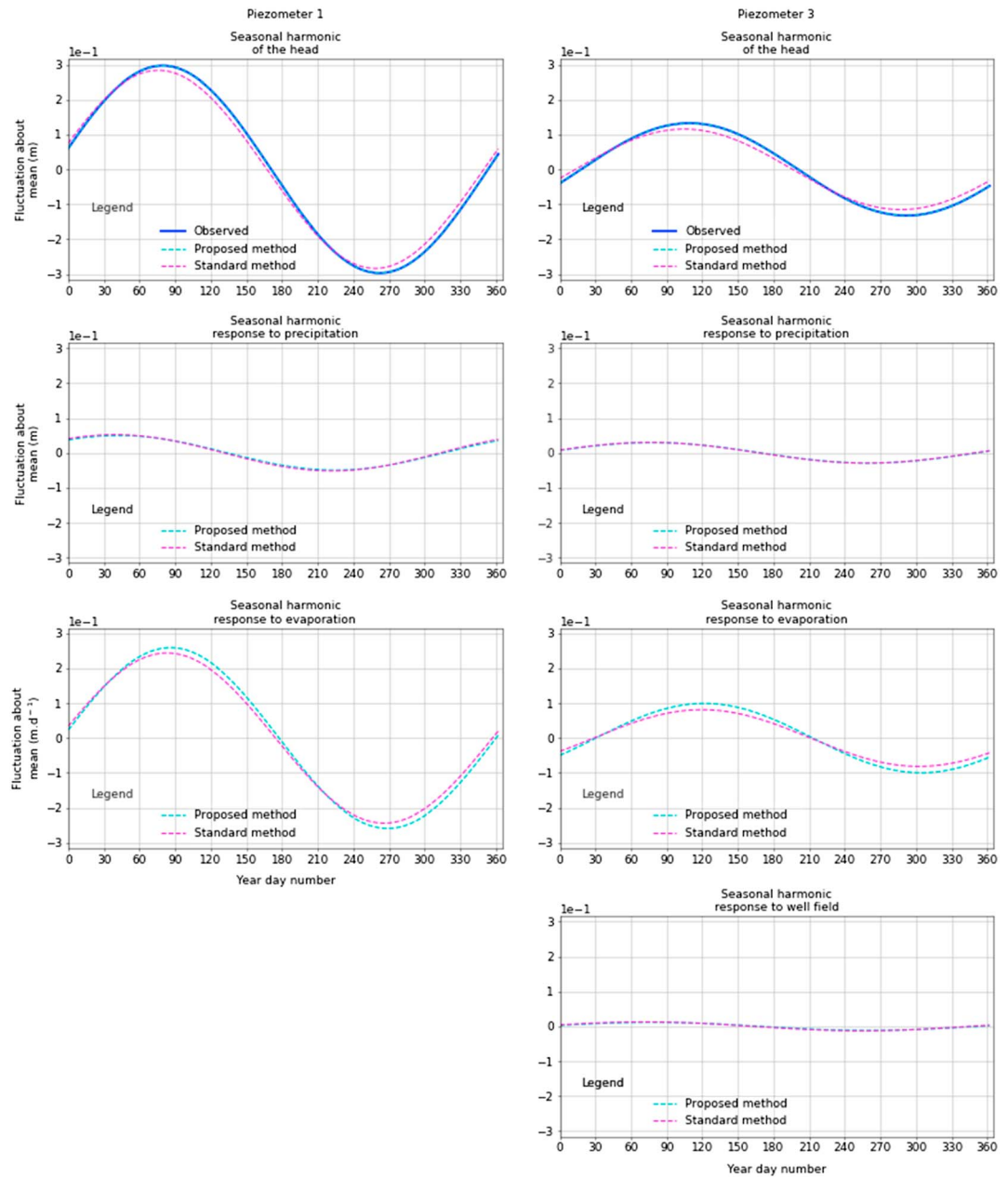
Figure 5. Comparison of the seasonal harmonics obtained with the proposed and standard methods.

parameters with a soft constraint (e.g., a range) by penalizing the objective function based on the extent that the condition is not met. In both approaches, the uncertainty of the seasonal harmonic may be taken into account in either assigning weights in the multiobjective optimization or in penalizing the objective function when applying a soft constraint, but this is the topic of further research.

5.5. Recharge Estimation by the Chloride Mass Balance Method

The recharge estimates obtained from time series analysis are compared with recharge estimates obtained with the saturated zone chloride mass balance method, assuming that the chloride in the groundwater is exclusively of atmospheric origin (rainwater and dry deposition; e.g., Allison & Hughes, 1978; Eriksson & Khunakasem, 1969; Simmers, 1988). In the present case study, this condition is reasonable because infiltration from surface water, chloride dissolution of minerals in the soil matrix, and chloride from anthropogenic
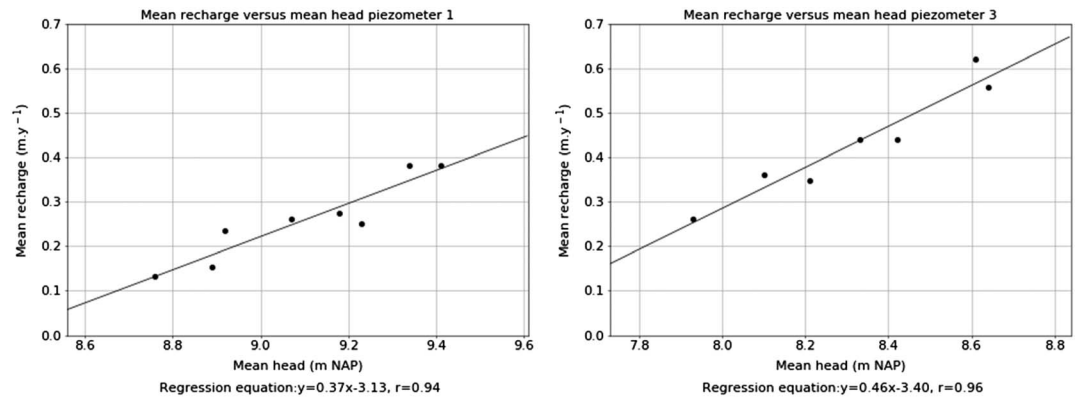
Figure 6. Estimated recharge with the proposed method over different time periods for piezometers 1 and 3 and best fit straight line.

sources can all be neglected. Furthermore, chloride originating from vegetation decomposition can be assumed to be entirely recycled during the growing season.

Under steady state conditions, the atmospheric chloride deposition flux equals the vertical chloride flux arriving at the groundwater table at the bottom of the root zone:

$$\overline{P}[Cl]_a = \overline{R}[Cl]_{gw} \tag{32}$$

where $\overline{P}$ and $\overline{R}$ are the mean precipitation and recharge rates $[LT^{-1}]$, respectively; $[Cl]_a$ is the mean concentration of atmospheric chloride (including dry deposition) $[ML^{-1}]$; and $[Cl]_{gw}$ is the mean chloride concentration in the groundwater at the groundwater table $[ML^{-1}]$.

The atmospheric chloride concentration in the Netherlands may be computed from the chloride concentration of the precipitation $[Cl]_p$ as (Ridder et al., 1984):

$$[Cl]_a = \frac{[Cl]_p}{f_{dp}} \tag{33}$$

where f_{dp} equals 0.83 with standard deviation of 0.10, which is applicable for open field deposition rates (Ridder et al., 1984). The chloride concentration of the precipitation is taken as the average of the three closest stations of the Dutch National Precipitation Chemistry Monitoring Network (van der Swaluw et al., 2010), which equals 1.9 mg/L with a standard deviation of 0.3 mg/L. The mean recharge can now be computed as

$$\overline{R} = \frac{\overline{P}[Cl]_p}{f_{dp}[Cl]_{gw}} \tag{34}$$

Chloride concentrations where measured in a monitoring well (code B28C0263) situated in a heather field at the western side of the ridge of Salland (Figure 2). The well is screened approximately 2 m below the highest measured water table and measurements were taken at four times between 1982 and 1995. Measured chloride concentrations are assumed to represent a mixture of the rainfall of the 2 years prior to the sampling date (based on a recharge of approximately 300 mm/year and a porosity of 0.3), so that the value of $\overline{P}$ in (34) is the mean precipitation of the 2 years prior to the sampling date.

The recharge is estimated for four 2-year periods based on four chloride measurements (Table 6). A confidence interval for the estimated recharge is generated by a Monte Carlo simulation where all variables were assumed to follow a Normal distribution centered on

Table 5
Uncertainty in the Seasonal Harmonic of the Different Time Series

Time series	Amplitude with relative standard deviation	Time-lag with standard deviation (days)
Piezometer 1	0.30 m [rel. SD = 2.3%]	340 [SD = 1.5]
Piezometer 2	0.30 m [rel. SD = 2.7%]	325 [SD = 1.5]
Piezometer 3	0.13 m [rel. SD = 6.0%]	3 [SD = 4.0]
Piezometer 4	1.00 m [rel. SD = 10.0%]	41 [SD = 5.0]
Piezometer 5	0.10 m [rel. SD = 8.0%]	66 [SD = 5.0]
Precipitation	3.8E−4 m/day [rel. SD = 26.0%]	211 [SD = 14.0]
Evaporation	1.5E−3 m/day [rel. SD = 1.0%]	255 [SD = 0.5]
Pumping	1.3E+3 m³/day [rel. SD = 3.0%]	246 [SD = 1.7]

Note. The uncertainty of the amplitude is given as the ratio of the estimated amplitude and the associated standard deviation; the uncertainty of the time-lag is expressed in days.

Table 6
Estimated Mean Yearly Recharge for 2-Year Periods Prior to Sampling Date and 95% Confidence Intervals

Sampling Date	[Cl] groundwater mg/l	Mean P (mm/year)	Estimated recharge (m/year)
2 October 1989	5.7	820	0.325 [0.230,0.460]
4 November 1993	6.7	920	0.310 [0.220,0.480]
15 September 1994	6.4	960	0.340 [0.240,0.480]
31 August 1995	5.5	995	0.410 [0.285,0.580]
Average			0.345 [0.240,0.500]

their measured values. Note that generating confidence intervals for recharge estimates obtained with the chloride mass balance is not common but has recently been advocated (e.g., Alcalá & Custodio, 2014, 2015; Crosbie et al., 2018). A standard deviation of 5% of the mean was used for the mean precipitation and for the measured groundwater chloride concentration in addition to the standard deviations of $[Cl]_p$ and f_{dp} mentioned above.

The mean recharge over the period 1989–1995, estimated with the chloride mass balance, equals 0.345 m/year, with an estimated confidence interval of [0.240,0.500]. The piezometer used for the chloride mass balance is located in an area with soil and vegetation cover similar to piezometers 3 and 4 but with a shallower groundwater table.

Considering the uncertainties associated with the chloride mass balance method and the difference in water table depth at the location of the piezometer considered, it is concluded that the results obtained using time series analysis are in reasonable agreement with the results obtained with the chloride mass balance.

6. Conclusion

Time series analysis of measured heads was applied to estimate the long-term mean recharge of water table aquifers in temperate climates where the seasonal trend of the evaporation results in a significant seasonal trend in the head. The proposed approach can be used to estimate the diffuse recharge with time series models that fit the observed heads as well as possible while requiring that the sum of the transformed seasonal harmonics present in the time series of the stresses equals the seasonal harmonic of the observed heads. In standard time series analysis, model parameters often show a high degree of correlation, leading to problems of equifinality which may result in poor and unreliable recharge estimates. Taking into account the seasonal harmonic of the observed heads as additional constraint results in more reliable and physically meaningful recharge estimates.

The proposed method is applied to head observations obtained from piezometers situated on and around the ice-pushed sand ridge of Salland in the Netherlands, using the best estimate of the seasonal harmonics of the observed time series. Recharge estimates over different time periods yield consistent results; the estimated mean recharge is linearly related to the mean head in the time period. A comparison with the saturated zone chloride mass balance yields recharge estimates of comparable magnitude.

There are four major requirements for application of the proposed method. First, the seasonal harmonic of the observed series can be estimated accurately. Second, the response of the system to recharge does not change over time, which precludes areas with significant land use changes or areas where the draining conditions of the aquifer are altered. Third, the aquifer system must be sufficiently linear. This condition can be considered as fulfilled when good model fits are obtained. And fourth, runoff is negligible or quantifiable.

The proposed method of time series analysis allows for the estimation of time-averaged diffuse recharge that can be used in groundwater modeling or catchment water balances. Where the density of piezometers is large, like in the Netherlands, the method opens the possibility to estimate the recharge at many points, which can be interpolated to generate a recharge map; such a map was generated by Alcalá and Custodio (2014) for Spain or Crosbie et al. (2018) for parts of Australia, using the chloride mass balance method.

Appendix A

In this appendix, a derivation of equations (19) and (20) is given. The seasonal harmonic (17) is written as the real part of a complex function:

$$y(t) = Ae^{i\omega(t-T)} \tag{A1}$$

The response of the seasonal harmonic is obtained from the convolution as

$$\widetilde{y}(t) = \int_0^\infty y(t-\tau)\theta(\tau)d\tau \tag{A2}$$

Substitution of (A1) for $y(t)$ and (9) for θ gives

$$\widetilde{y}(t) = AM \int_0^\infty e^{-i\omega(t-T-\tau)} \frac{a^n \tau^{n-1}}{\Gamma(n)} e^{-a\tau} d\tau \tag{A3}$$

Defining a new variable

$$\beta = a - i\omega \tag{A4}$$

and rearrangement of terms give

$$\widetilde{y}(t) = AM \frac{a^n e^{-i\omega(t-T)}}{\Gamma(n)} \int_0^\infty e^{-\beta\tau} \tau^{n-1} d\tau \tag{A5}$$

which may be rewritten as

$$\widetilde{y}(t) = AM \frac{a^n e^{i\omega(t-T)}}{\Gamma(n)} \frac{1}{\beta^n} \int_0^\infty (\beta\tau)^{n-1} e^{-\beta\tau} d(\beta\tau) \tag{A6}$$

The integral equals the gamma function of n (e.g., Abramowitz & Stegun, 1964) so that

$$\widetilde{y}(t) = AM \frac{a^n e^{-i\omega(t-T)}}{\beta^n} \tag{A7}$$

Replacing β again by $a - i\omega$ and division of the numerator and denominator by a^n give

$$\widetilde{y}(t) = \frac{AM}{\left(1 - i\frac{\omega}{a}\right)^n} e^{-i\omega(t-T)} \tag{A8}$$

Rewriting the denominator as

$$\left(1 - i\frac{\omega}{a}\right)^n = \left(1 + \frac{\omega^2}{a^2}\right)^{\frac{n}{2}} e^{-in\arctan\left(\frac{\omega}{a}\right)} \tag{A9}$$

And combining terms gives

$$\widetilde{y}(t) = \frac{AM}{\left(1 + \frac{\omega^2}{a^2}\right)^{\frac{n}{2}}} e^{-i\omega\left(\left(t - T - \frac{n}{\omega}\arctan\frac{\omega}{a}\right)\right)}. \tag{A10}$$

Comparison of (A10) with (18) gives equations (19) and (20).

Availability of Data and Materials

Water Resources Research

References

Abramowitz, M., & Stegun, I. A. E. (1964). *Handbook of mathematical functions* (p. 1046). New-York: Dover Publications.

Alcalá, F. J., & Custodio, E. (2014). Spatial average aquifer recharge through atmospheric chloride mass balance and its uncertainty in continental Spain. *Hydrological Processes*, *28*(2), 218–236.

Alcalá, F. J., & Custodio, E. (2015). Natural uncertainty of spatial average aquifer recharge through atmospheric chloride mass balance in continental Spain. *Journal of Hydrology*, *524*, 642–661.

Allison, G., & Hughes, M. (1978). The use of environmental chloride and tritium to estimate total recharge to an unconfined aquifer. *Soil Research*, *16*(2), 181–195.

von Asmuth, J. R., & Bierkens, M. F. P. (2005). Modeling irregularly spaced residual series as a continuous stochastic process. *Water Resources Research*, *41*, W12404. https://doi.org/10.1029/2004WR003726

von Asmuth, J. R., Maas, K., & Bierkens, M. F. P. (2002). Transfer function-noise modeling in continuous time using predefined impulse response functions. *Water Resources Research*, *38*(12), 1287. https://doi.org/10.1029/2001WR001136

von Asmuth, J. R., Maas, K., Knotters, M., Bierkens, M. F. P., Bakker, M., Olsthoorn, T. N., et al. (2012). Software for hydrogeologic time series analysis, interfacing data with physical insight. *Environmental Modeling & Software*, *38*, 178–190.

Baggelaar, P. K. (1988), Time series analysis in groundwater level decline studies: principle and example (in Dutch), H2O, 21, 443-450.

Bakker, M., Bartholomeus, R. P., & Ferré, T. P. A. (2013). Preface "Groundwater recharge: processes and quantification", *Hydrology and Earth System Sciences*, *17*(7), 2653-2655.

Berendrecht, W. L., Heemink, A. W., van Geer, F. C., & Gehrels, J. C. (2006). A non-linear state space approach to model groundwater fluctuations. *Advances in Water Resources*, *29*(7), 959–973.

Besbes, M., & de Marsily, G. (1984). From infiltration to recharge: Use of a parametric transfer function. *Journal of Hydrology*, *74*, 271–293.

Beven, K. (1993). Prophecy, reality and uncertainty in distributed hydrological modeling. *Advances in Water Resources*, *16*(1), 41–51.

Crosbie, R. S., Binning, P., & Kalma, J. D. (2005). A time series approach to inferring groundwater recharge using the water table fluctuation method. *Water Resources Research*, *41*, W01008. https://doi.org/10.1029/2004WR003077

Crosbie, R. S., Peeters, L. J. M., Herron, N., McVicar, T. R., & Herr, A. (2018). Estimating groundwater recharge and its associated uncertainty: Use of regression kriging and the chloride mass balance method. *Journal of Hydrology*, *561*, 1063–1080.

Cuthbert, M. O. (2010). An improved time series approach for estimating groundwater recharge from groundwater level fluctuations. *Water Resources Research*, *46*, W09515. https://doi.org/10.1029/2009WR008572

De Bruin, H. A. R. (1987). From Penman to Makkink, paper presented at Evaporation and weather, TNO Comitee on Hydrological Research.

Doble, R. C., & Crosbie, R. S. (2017). Review: Current and emerging methods for catchment-scale modelling of recharge and evapotranspiration from shallow groundwater. *Hydrogeology Journal*, *25*(1), 3–23.

Efstratiadis, A., & Koutsoyiannis, D. (2010). One decade of multi-objective calibration approaches in hydrological modelling: A review. *Hydrological Sciences Journal*, *55*(1), 58–78.

Eriksson, E., & Khunakasem, V. (1969). Chloride concentration in groundwater, recharge rate and rate of deposition of chloride in the Israel Coastal Plain. *Journal of Hydrology*, *7*(2), 178–197.

Euser, T., Winsemius, H. C., Hrachowitz, M., Fenicia, F., Uhlenbrook, S., & Savenije, H. H. G. (2013). A framework to assess the realism of model structures using hydrological signatures. *Hydrology and Earth System Sciences*, *17*(5), 1893–1912.

van Geer, F. C., & Zuur, A. F. (1997). An extension of Box-Jenkins transfer/noise models for spatial interpolation of groundwater head series. *Journal of Hydrology*, *192*(1–4), 65–80.

Gehrels, J. C., van Geer, F. C., & de Vries, J. J. (1994). Decomposition ot groundwater level fluctuations using transfer modelling in an area with shallow to deep unsaturated zones. *Journal of Hydrology*, *157*, 105–138.

Healy, R., & Cook, P. (2002). Using groundwater levels to estimate recharge. *Hydrogeology Journal*, *10*(1), 91–109.

Healy, R. W. (2012). *Estimating groundwater recharge*. Cambridge, UK: Cambridge University Presss.

Heppner, C. S., & Nimmo, J. R. (2005). A computer program for predicting recharge with a master recession curve, U.S. Geological Survey.

Hill, M. C. (1998). Methods and guidelines for effective model calibration. Rep. Open-file Rep 98-4005, USGS.

Hrachowitz, M., Fovet, O., Ruiz, L., Euser, T., Gharari, S., Nijzink, R., et al. (2014). Process consistency in models: The importance of system signatures, expert knowledge, and process complexity. *Water Resources Research*, *50*, 7445–7469. https://doi.org/10.1002/2014WR015484

Iman, R. L., Helton, J. C., & Campbell, J. E. (1981). An approach to sensitivity analysis of computer models: Part I—Introduction, input variable selection and preliminary variable assessment. *Journal of Quality Technology*, *13*(3), 174–183.

Jones, E., Oliphant, E., & Peterson, P. (2001). SciPy: Open source scientific tools for Python, edited.

Koutsoyiannis, D. (2010). One decade of multi-objective calibration approaches in hydrological modeling: A review AU-Efstratiadis, Andreas. *Hydrological Sciences Journal*, *55*(1), 58–78.

Manzione, R., Wendland, E., & Tanikawa, D. (2012). Stochastic simulation of time-series models combined with geostatistics to predict water-table scenarios in a Guarani Aquifer System outcrop area, Brazil. *Hydrogeology Journal*, 1–11.

Meinzer, O. E. (1923). The occurrence of ground water in the United States, with a discussion of principles, Report Rep. 489 (373 pp.). Washington, DC.

Moré, J. J., Garbow, B. S., & Hillstrom, K. E. (1980). User guide for MINPACK-1, Argonne National Laboratory Argonne, Illinois, USA.

Nash, J. E., & Sutcliffe, J. V. (1970). River flow forecasting through conceptual models. Part I—A discussion of principles. *Journal of Hydrology*, *10*(3), 282–290.

Nimmo, J. R., Horowitz, C., & Mitchell, L. (2015). Discrete-storm water-table fluctuation method to estimate episodic recharge. *Groundwater*, *53*(2), 282–292.

Obergfell, C., Bakker, M., & Maas, K. (2016). A time-series analysis framework for the flood-wave method to estimate groundwater model parameters. *Hydrogeology Journal*, 1–13.

Peterson, T. J., & Western, A. W. (2014). Nonlinear time-series modeling of unconfined groundwater head. *Water Resources Research*, *50*, 8330–8355. https://doi.org/10.1002/2013WR014800

Ridder, T. B., Baard, J. H., & Buishand, T. A. (1984). The influence of sampling methods and analysis techniques on measured chemical concentrations in rain water (in Dutch), De Bilt, Netherlands.

Scanlon, B. R., Healy, R. W., & Cook, P. G. (2002). Choosing appropriate techniques for quantifying groundwater recharge. *Hydrogeology Journal*, *10*(1), 18–39.

Shapoori, V., Peterson, T. J., Western, A. W., & Costelloe, J. F. (2015). Decomposing groundwater head variations into meteorological and pumping components: a synthetic study. *Hydrogeology Journal*, 1–18.

Simmers, I. (1988). Numerical and conceptual models for recharge estimation in arid and semi-arid zones. In I. Simmers (Ed.), *Estimation of natural groundwater recharge*, *NATO ASI Series C* (Vol. 222, pp. 301–311). Dordrecht, Netherlands: D. Reidel Publication Company.

van der Swaluw, E., Asman, W. A. H., & Hoogerbrugge, R. (2010). The Dutch National Precipitation.

Yuen, K. V. (2010). *Bayesian methods for structural dynamics and civil engineering*. Singapore: John Wiley & Sons (Asia) Pte Ltd.